ISSN 1392–1207. MECHANIKA. 2017 Volume 23(6): 923–930

Temperature Effect on the Kinetic Alumina Layer Growth on 5086 Aluminum Substrate

A. RAID*, S. PAVAN, V. FRIDRICI**, C. POILÂNE***, Ph. KAPSA****

**LSCMI, Mechanical Engineering Faculty, University of Sciences and Technology Oran Mohamed Boudiaf BP 1505 El M'Naouer 31000, Oran-Algeria. E-mail: bousourai@yahoo.fr*
***Laboratory of Tribology and Systems Dynamics (LTDS), UMR 5513, 36 Avenue Guy de Collongue, 69134 Ecully, Cedex, France. E-mail: Sophie.Pavan@ec-lyon.f; E-mail: Vincent.Fridrici@ec-lyon.fr; E-mail: Philippe.Kapsa@ec-lyon.fr*
****Normandie Univ, Esplanade de la Paix, F-14032 Caen, Cedex 5, France, UNICAEN, CIMAP, F-14050 Caen, France, ENSICAEN, F-14050 Caen, France, CNRS, UMR 6252, F-14050 Caen, France, CEA, UMR 6252, F-14050 Caen, France, E-mail: christophe.poilane@unicaen.fr*

crossref http://dx.doi.org/10.5755/j01.mech.23.6.16309

1. Introduction

Nowadays, the surface finishing becomes a greater part of final product and the coating plays an important part to enhance adherence properties. In anodization process, the current flows through an electrolyte in which aluminium sheet is used as anode. A thick film of aluminium oxide is built up on this substrate surface. Various parameters determine the structure and the properties of a formed porous anodic alumina (PAA) [1, 2]. The layer is uniform and presents a higher corrosion and abrasion resistance to those of the aluminum. The most important electrolytes are sulfuric acid (SAA: H_2SO_4), chromic acid (CAA: H_2CrO_4), phosphoric acid (PAO: H_3PO_4), boric acid (BAAO: H_3BO_3) and oxalic acid (OAA: HOOC-COOH) [3]. A mixed of different acids is used as electrolyte in the aerospace industry. Porous alumina films consist in two layers: a thin barrier of oxide in contact with the metal and a thick porous layer. The anodic oxide exhibits good electrical resistance, which is correlated to the oxide thickness. Aluminum oxide is very resistant to electric current and the current density decreases with time anodizing. An appropriate anodization parameters control allows obtaining good results in terms of porous structure regularity [4]. The applied voltage, the current density, the texture, microstructure of aluminum substrate and the temperature affect the pores distribution as a honeycomb during the anodizing process [5-7].

Current distribution was modeled by Akolkar et al. [8] in stirred H_2SO_4 electrolyte at different voltages and temperatures for various anodizing times; they showed that the major resistivity resides in the sub-layer.

Sulka and Parkola [9] obtained good results for anodizing parameters control at 25 V for a temperature of 1°C. The anodic oxide film formed at 58°C exhibits lower dielectric properties compared with the amorphous oxide films at 8°C and 25°C [10].

Several authors showed the interest of temperature on the courant behavior [11, 12]. A difference, of 20°C between low temperature (0°C) and room temperature, modifies the alumina layer kinetic growth. A local difference of 5°C generates cracks into the oxide layer at the interface [13]. Aerts et al. [14] quantified the porosity and the pores dimension with temperature whereas Sulka and Parkola [15] and Araoyinbo et al. [16] analyzed the effect of applied anodizing voltage. Fratila-Apachitei et al. [17] showed the effect of the convective regime on electrode temperature at 65°C as on oxide layer growth. Vrublevsky et al. [18] confirmed the change in the growth mechanism of porous alumina for a tension above 55 V by the break in the curves of anodizing voltage. They used a temperature of 50°C for chemical dissolution of the oxide, and then the temperature reaches rapidly 60°C under free convection which enhances local oxide dissolution resulting in non-uniform thickness. Aerts et al. [19] studied the anode electrochemical behavior, the oxide layer morphology with the temperature variation of anode and electrolytic solution.

Temperature close to the boiling point (96°C), usually undertaken for the sealing process, involves secondary reactions in anodized layer [20-21].

Assessment of mechanical properties such as hardness and Young's modulus is necessary to analyze the mechanical behavior of coating layers under static or dynamic conditions [22]. The accurate determination of the elasticity modulus is possible for massive and homogeneous materials with Vickers hardness tests. However, it is often difficult to achieve it for thin films with heterogeneous properties. Nano-indentation tests are used for mechanical characterization of thin film [23–26].

2. Experimental

2.1. Sample's preparation

The experiments were conducted with 5086 aluminium alloy (4.9 wt % Mg) as substrate with chemical composition given in Table 1.

Table 1
Chemical composition of Al 5086 H111 (mass %)

Si	Fe	Cu	Mn	Mg	Cr	Zn	Ti+Zr
Max 0.40	Max 0.40	Max 0.1	0.40 1.00	4.00 4.90	0.05 0.25	Max 0.25	Max 0.15

Samples are cut out with precision blade (ISOMET 4000 BUEHLER) under lubrication. Final dimensions of samples are 120 mm x 25 mm x 2.5 mm. Before anodiz-

ing, polishing of twelve surface specimens was grounded successively with silicon carbide papers from 120 to 1200, diamond paste 1 µm and alumina 0.4 µm to reach a mirror state with 0.1 µm roughness. Then, specimens were cleaned in an ultrasonic acetone bath during 15 min then rinsed with distilled water.

2.2. Anodization

We choose a diluted H_2SO_4 solution (SAA, 20 % mass) largely used in industry to obtain a hard layer [27]. The hard anodization process in sulfuric acid at low temperature easily develops an oxide layer much thicker than natural barrier, up to 150 µm during few hours. Directly built and strongly bonded on the aluminium, alumina is a passive oxide film barrier in the electrolyte with pH range from 4 to 8.

A special electrodes configuration was adopted to minimize the electrolyte resistance. The aluminium anode is placed at 2 mm from the borders lead cathode shaped in V as illustrated in Fig. 1. The anodization SAA was performed in 1 L glass beaker cooled by a circulating machine (Lauda Circulator Programmable C6). Cooling temperatures ranging between 16°C to 21°C are used for specimens at room (RT) and between -1°C to 4°C for the lowest temperatures (LT). A magnetic stirrer at 500 rpm is used to prevent localized temperature concentration. After anodizing, the specimens were only rinsed with distilled water and dried with compressed air without sealing to conserve the layers in their initial states.

The anodization time was set at 30 min, 60 min, 120 min, 180 min, 240 min and 300 min with an initial current of 1.4 A corresponding to voltages of 14 and 18 V respectively for both cooling temperatures. For long anodization times (beyond to 30 min) we consider that the thermal equilibrium is well established between the electrolyte and the electrodes. The solution being vigorously stirred, the difference in temperature between the oxide and the substrate, which presents a high thermal conductivity, is negligible [19].

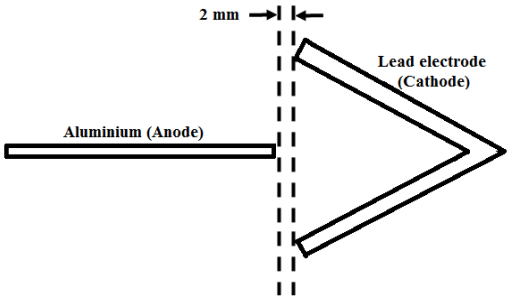

Fig. 1 Configuration of electrodes

3. Results and discussions

Current, temperature and voltage evolution are automatically recorded according to time. The voltage evolution according to times at low and room temperature are gathered in Fig. 2 for an initial courant of 1.4 A. The effect of anodization time is significant on tension at low temperature. We observed a difference ranging from 3V to 8 V during anodization between low and room temperature. The current decreases more rapidly at low temperature than at room temperature as shown in Figs. 3 and 4. This result well agrees with results given in [10].

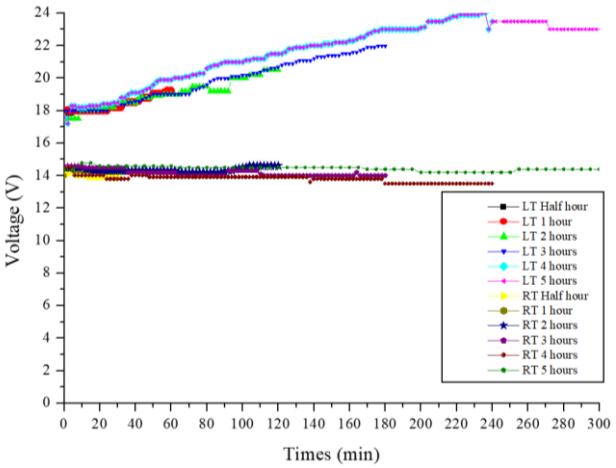

Fig. 2 Voltage *vs* anodizing time at low and room temperature

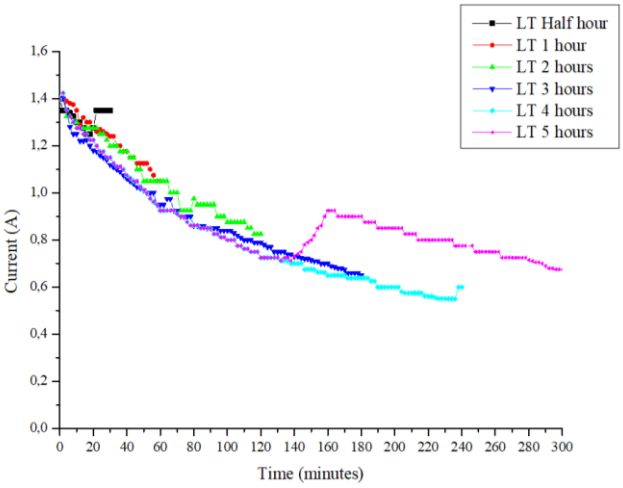

Fig. 3 Current *vs* anodizing time at low temperature

Qualitatively, the Fig. 5 shows a large colors range, each one corresponding to a given thickness and the alumina layer growth with the anodizing time and temperature. Colors ranging are from light to dark gray for tests at room temperature corresponding to layers with thickness lower than 80 µm and from light brown to very dark. At low temperatures the thickness can reach 150 µm.

The specimen cross section was examined by microscopy where the thickness was directly measured, Fig. 6.

Hard anodizing in sulphuric acid at low temperature forms a thicker layers oxide than those at room temperature, Fig 7.

The difference in thickness is particularly observed for time up to 60 min and it is not recommended to continue anodizing after 120 min at room temperature since the oxidation is balanced by a simultaneous ions reduction presents in solution. This drawback is not noted at low temperature which explains the ability to make thick anodized layer by such a way. For the fifth specimen at

low temperature (5 hours, LT), we have voluntarily stopped the cooling after 120 min anodizing.

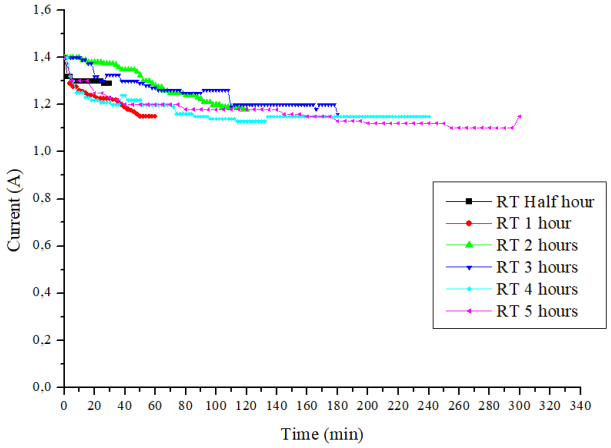

Fig. 4 Current *vs* anodizing time at room temperature

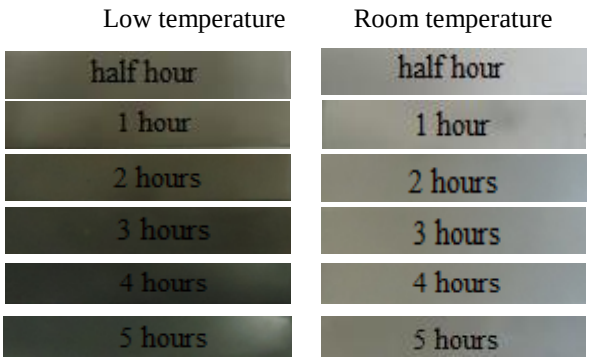

Fig. 5 Colors adopted by the samples for different anodization times at low and room temperature

We noted a sudden increase of the current that is due to the rise of the current reduction which is responsible of the oxide dissolution.

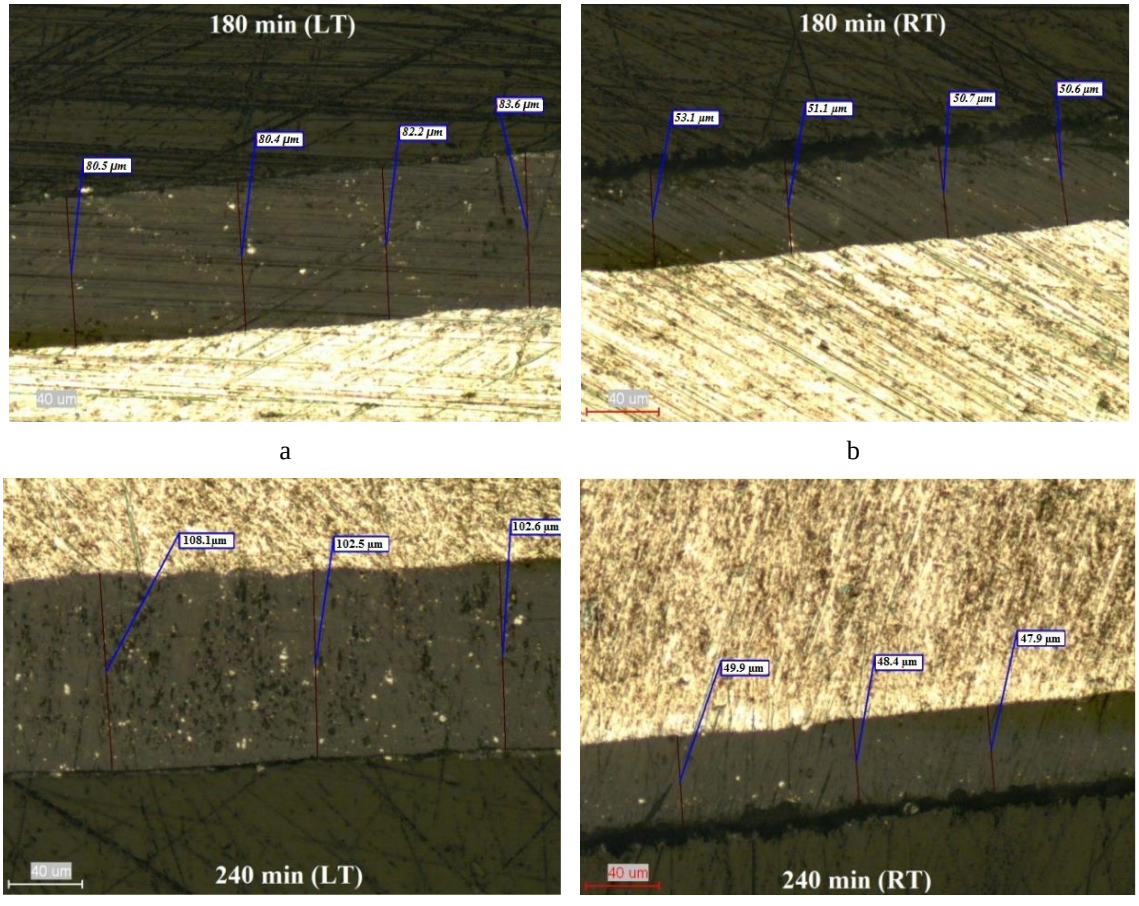

a b

c d

Fig. 6 Cross section of alumina layers at low (LT) and room temperature (RT) respectively for 180 and 240 min anodizing: (a) 180 min (LT), (b) 180 min (RT), (c) 240 min (LT) and (d) 240 min (RT)

Thus, this promotes defects in the oxide film and the current curve is close to the current room temperature, Fig. 3. All current curves versus of time show regularly spaced fluctuations; two cases are considered:

1. A local increase in temperature leads to the dissolution of the oxide and consequently to a decrease in the layer growth kinetics.
2. During growth, a difference between the densities of alumina and aluminum substrate, generates cracks during anodizing, Fig. 9, a. Cracks can be deep, Fig. 9, b. Then, the exposure of the substrate aluminum in contact with the electrolyte develops a high current density, because the anodic surface (aluminum) is very little in regard with the large cathode surface (alumina).

Fig. 8 shows porosities in the cross section layer at low and room temperature, the effect of cold sulfuric acid electrolyte enhances the pores formation. At the initial

anodizing state and at the surface or immediately close to the substrate, Mg_5Al_8 precipitates generate magnesium cation which migrates across the oxide under electric field faster than aluminium [28]. During anodizing formation of alumina and for long time, the precipitates are trapped in the oxide and the magnesium content in Mg_5Al_8 particles, highly soluble in the acid electrolyte, forms pores through the cross section and in regions called stains [29].

A detailed observation of color evolution at LT shows a slight decrease in blackness for the fifth sample, Fig. 5.

Fig. 10 illustrates the hardness evolution according to anodizing time. The measurement was made on the top of coating surface. The hardness of low temperature alumina is more important, the maximal value is reached at two hours, after which there is no need to extend the anodizing process.

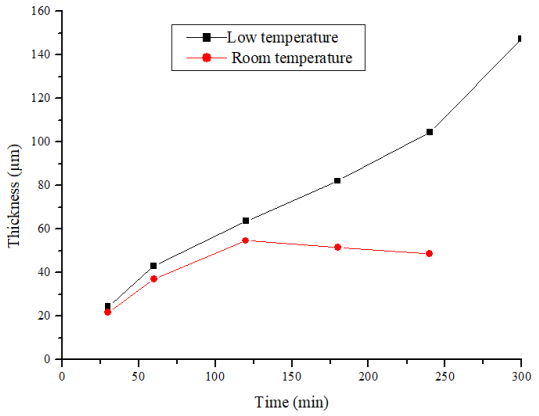

Fig. 7 Thickness evolutions against time anodizing for room and low temperature

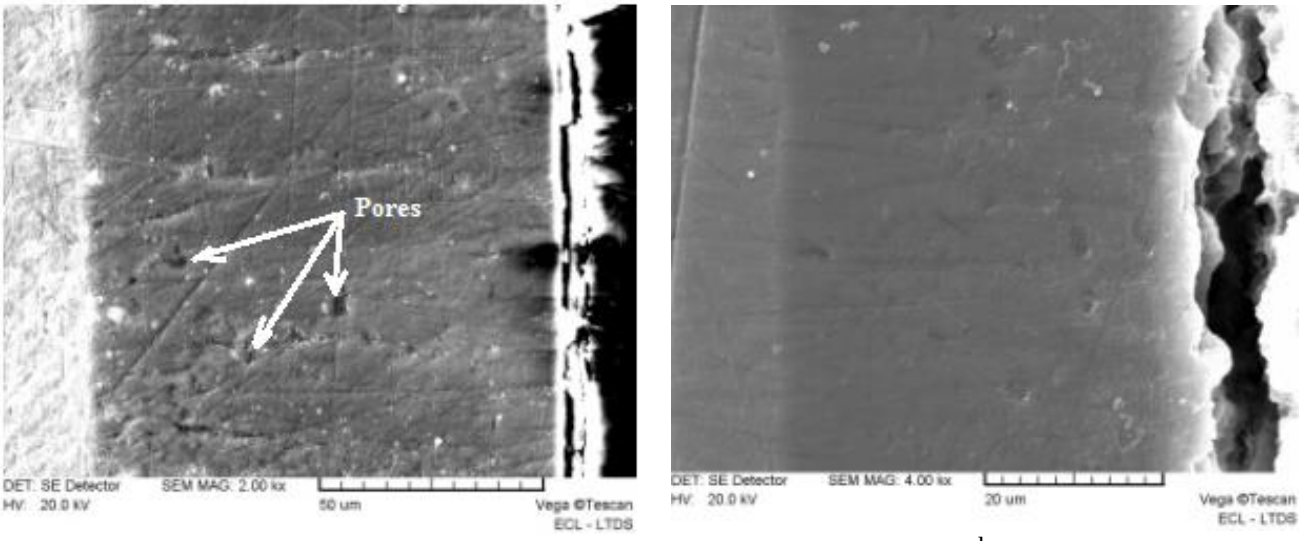

a b

Fig. 8 SEM micrographs of the 240 min anodized layer. a – low temperature, b – room temperature

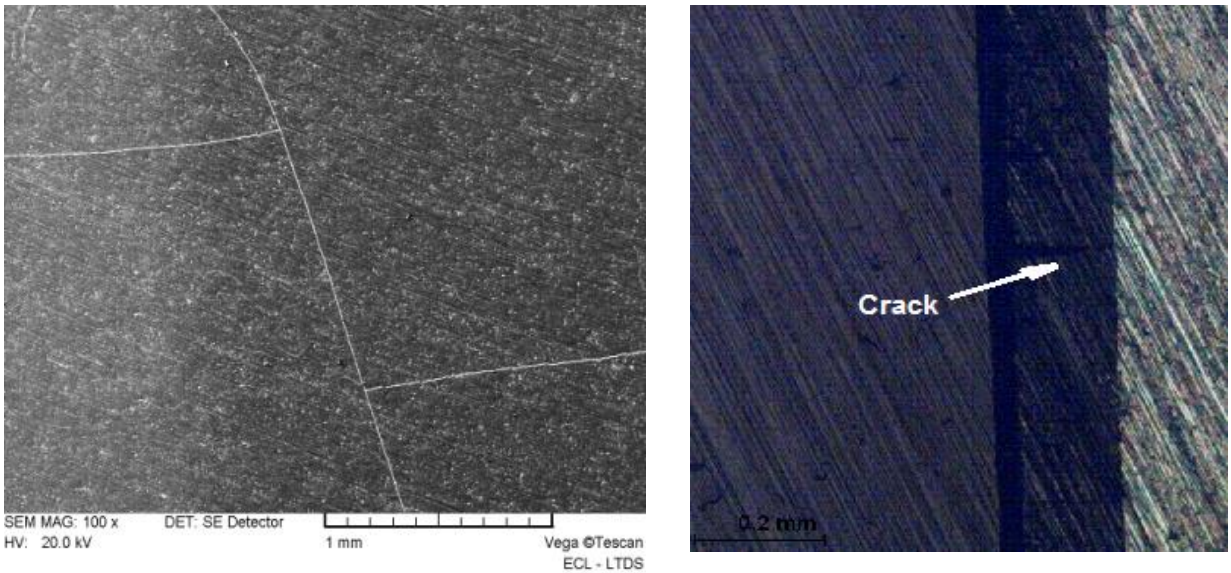

a b

Fig. 9 SEM micrographs of the 300 min anodized specimen at low temperature: a – cracks on the surface, b – crack in the cross-section

For the aim to assess the mechanical proprieties of both aluminium and oxide layer, a nano-indentations was performed on a row according to an angle of 20 °C with oxide-aluminum interface. The distances between

imprints into the layer are 15 µm through thickness and 40 µm in the longitudinal direction. The tests were conducted at room temperature on XP nano-indenter with a Berkovich indenter. A maximum load of 450 mN was applied.

Before and after tests nanoindentation, indentations are performed on a reference sample of silica, for two reasons in order to:

- Establish the defect of the indenter tip (Berkovich) used for the calculations of hardness and elastic's modulus.
- Check the mechanical properties on a silica sample.

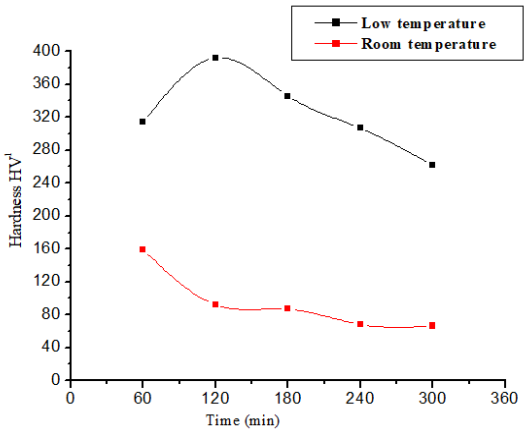

Fig. 10 Hardness against hard anodizing time on the layer surface

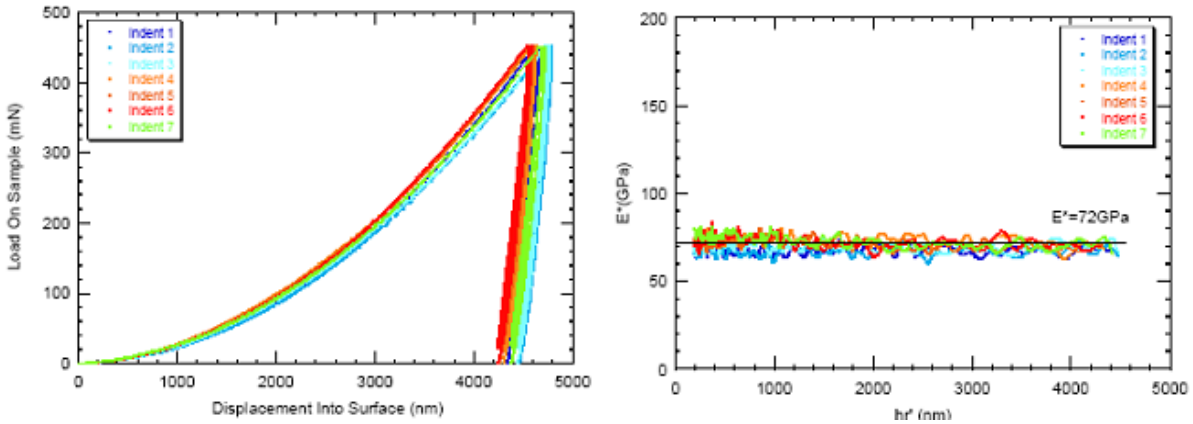

a b

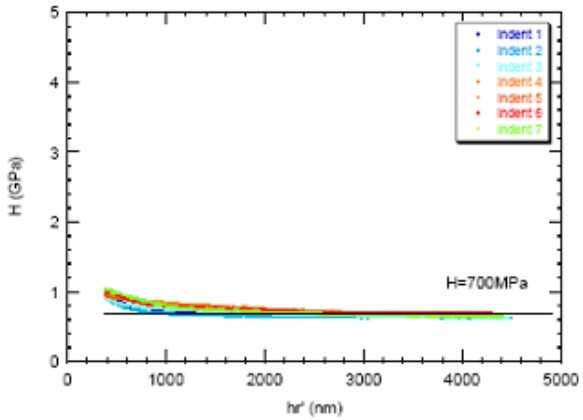

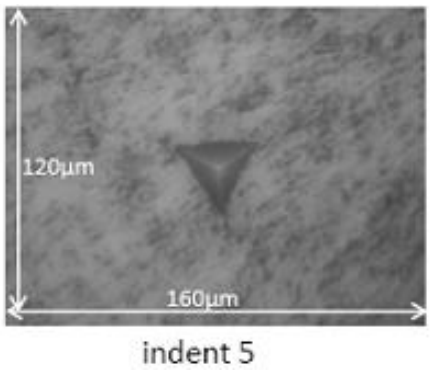

c d

Fig. 11 a – Loading- unloading curves, b – Reduced Young modulus evolutions, c – hardness evolutions and d – the fifth indent imprint measured on aluminum substrate by nano-indentation

The Fig. 11 represents respectively loading-unloading curves, the reduced Young's modulus evolution, hardness and one example of imprint obtained for aluminium subtract. We remark that the substrate exhibits homogeneous mechanical properties. The average hardness and the reduced Young modulus values are, 700 MPa and 72 GPa, respectively [30]. Fig. 12 represents the loading-unloading curves, the evolution of reduced Young's modulus and hardness, and the imprint series in the alumina layer. Nano-indentation analysis shows heterogeneity in the mechanical properties during layer growth, Fig. 13.

The reduced Young modulus and the hardness vary respectively from 80 GPa to 40 GPa and from 1 GPa to 4 GPa from the interface to the oxide outer limit.

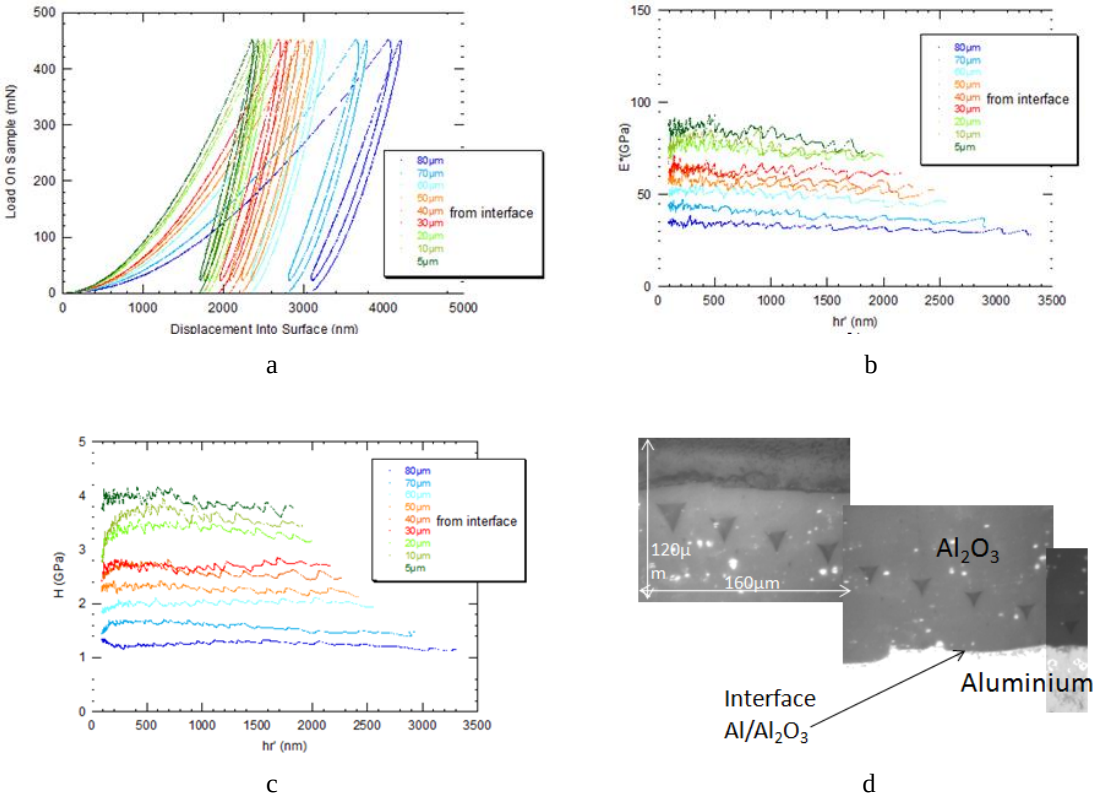

a b c d

Fig. 12 a – Loading- unloading curves, b – reduced Young modulus, c – hardness evolutions and d – imprints measured on oxide layer by nano-indentation

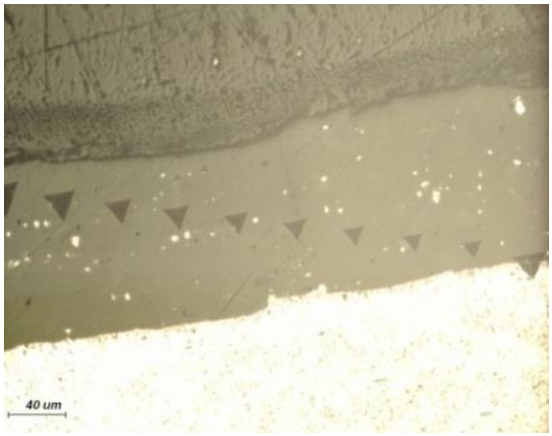

Fig. 13 Imprints on the oxide layer and on the interface

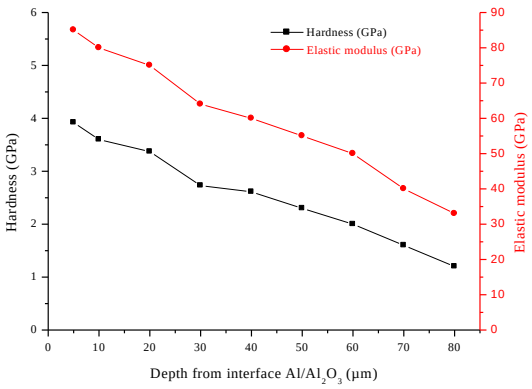

Fig. 14 Average of the Hardness and the elastic modulus against depth from interface Al/Al_2O_3

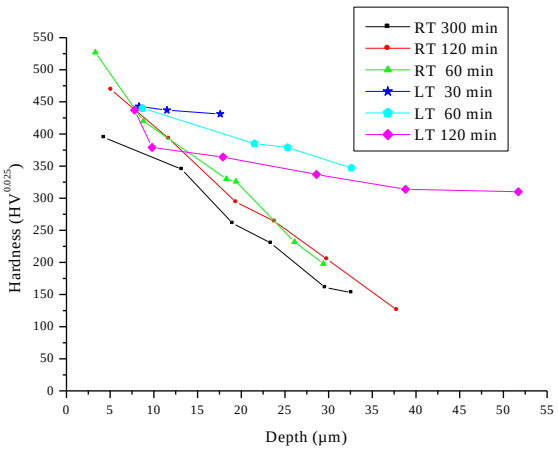

Fig. 15 Cross section hardness variation against depth for 1, 2 and 5 hours at room temperature and from half to five hours at low temperature

The average hardness and Young's modulus evolution according to depth are presented in Fig. 14. It is clear that the alumina is heterogonous in terms of mechanical properties through the oxide cross section. That is due to defect induced during the pores growth generated by the anodizing process.

The evolution of hardness with the thickness oxide is similar whatever the anodization time. In the Fig. 15, the origin of the depth scale is the aluminium interface. The hardness decreases with the depth but this is particularly more quickly according to RT anodization.

4. Conclusion

In this study we showed qualitatively the temperature effect and layers color correlation with the thickness. For all anodizing times at room temperature the voltage was constant but the current decreases according to the alumina layer thickness growth. At low temperature, the forced convection of the electrolyte improves the layer's growth and avoids a local temperature rise. In all case, low temperatures enhance layer's thickness growth with high mechanical properties than those the room temperature alumina witch the layer thickness is limited in time. Nanoindentation tests illustrate the heterogeneous nature of alumina layer at room temperature.

References

1. **Bensalah, W.; Feki, M.; Wery M.; Ayedi, H.F.** 2010. Thick and Dense Anodic Oxide Layers Formed on Aluminum in Sulphuric Acid Bath, J. Mater. Sci. Technol. 26(2): 113-118. https://doi.org/10.1016/S1005-0302(10)60018-7.
2. **Montero-Moreno, J. M.; Sarret, M.; Muller, C.** 2007. Influence of the aluminum surface on the final results of a two-step anodizing, Surf. Coat. Technol. 201: 6352–6357. https://doi.org/10.1016/j.surfcoat.2006.12.003.
3. **Dasquet, J.; Caillard, D.; Bonino, J.; Bes, R.** 2001. Characterization of the protective effect of aluminium surface treatments by d.c. and a.c. measurements, J. Mater. Sci. 36 3549–3555. https://doi.org/10.1023/A:1017997003919.
4. **Ba, L.; Li**, **W.** 2000. Influence of anodizing conditions on the ordered pore formation in anodic alumina, J. Phys. D-Appl. Phys. 33 2527–2531. https://doi.org/10.1088/0022-3727/33/20/302.
5. **Kashi, M.; Ramazani, A.** 2005 The effect of temperature and concentration on the self-organized pore formation in anodic alumina, J. Phys. D-Appl. Phys. 38 2396–2399. https://doi.org/10.1088/0022-3727/38/14/015.
6. **Chowdhury, P.; Raghuvaran, K.; Krishnan, M.; Barshilia, H. C.; Rajam, K. S.** 2011. Effect of process parameters on growth rate and diameter of nano-porous alumina templates, Bull. Mat. Sci. 34: 423-427. https://doi.org/10.1007/s12034-011-0104-6.
7. **Choong-Soo Chi, Jong-Ho Lee, Insoo Kim, Han-Jun Oh**, 2015. Effects of Microstructure of Aluminum Substrate on Ordered Nanopore Arrays in Anodic Alumina, Journal of Materials Science & Technology 31: 751-758. https://doi.org/10.1016/j.jmst.2014.09.019.
8. **Akolkar, R.; Landau, U.; Kuo, H.; Wang, Y.** 2004. Modeling of the current distribution in aluminum anodization, J. Appl. Electrochem 34: 807– 813. https://doi.org/10.1023/B:JACH.0000035611.87036.36
9. **Sulka, G. D.; Parkola, K. G.** 2007. Temperature influence on well-ordered nanopore structures grown by anodization of aluminium in sulphuric acid, Electrochim. Acta 52: 1880–1888. https://doi.org/10.1016/j.electacta.2006.07.053.
10. **Chiu, R.; Chang, P.; Tung, C.** 1995. The effect of anodizing temperature on anodic oxide formed on pure al thin-films, Thin Solid Films 260: 47–53. https://doi.org/10.1016/0040-6090(94)06491-1.
11. **Vrublevsky, I.; Parkoun, V.; Schreckenbach, J.** 2005. Analysis of porous oxide film growth on aluminum in phosphoric acid using re-anodizing technique, Appl. Surf. Sci. 242: 333–338. https://doi.org/10.1016/j.apsusc.2004.08.034.
12. **Zhou, F.; Baron-Wiechec, A. S.; Garcia-Vergara, J.; Curioni, M.; Habazaki, H.; Skeldon, P.; Thompson, G. E.** 2012. Effects of current density and electrolyte temperature on the volume expansion factor of anodic alumina formed in oxalic acid, Electrochim. Acta 59: 186–195. https://doi.org/10.1016/j.electacta.2011.10.052.
13. **Goueffon, Y.; Mabru, C.; Labarrere, M.; Arurault, L.; Tonon, C.; Guigue, P.** 2009. Mechanical behavior of black anodic films on 7175 aluminium alloy for space applications, Surf. Coat. Technol. 204: 1013–1017, 36th International Conference on Metallurgical Coatings and Thin Films, San Diego, CA, APR 27-MAY 01.
14. **Aerts, T.; Dimogerontakis, T.; De Graeve, I.; Fransaer, J.; Terryn, H.** 2007. Influence of the anodizing temperature on the porosity and the mechanical properties of the porous anodic oxide film, Surf. Coat. Technol. 201: 7310–7317. https://doi.org/10.1016/j.surfcoat.2007.01.044.
15. **Sulka, G. D.; Parkola, K. G.** 2006. Anodising potential influence on well-ordered nanostructures formed by anodisation of aluminium in sulphuric acid, Thin Solid Films 515: 338–345. https://doi.org/10.1016/j.tsf.2005.12.094.
16. **Araoyinbo, A. O.; Noor, A. F. M.; Sreekantan, S.; Aziz, A.** 2010. Voltage effect on electrochemical anodization of aluminum at ambient temperature, Int. J. Mech. Mat. Eng. 5: 53–58.
17. **Fratila-Apachitei,** L**.; Apachitei, I.; Duszczyk, J.** 2006. Thermal effects associated with hard anodizing of cast aluminum alloys, J. Appl. Electrochem. 36: 481–486. https://doi.org/10.1007/s10800-005-9102-y.
18. **Vrublevsky, I.; Parkoun, V.; Sokol, V.; Schreckenbach, J.** 2004. Study of chemical dissolution of the barrier oxide layer of porous alumina films formed in oxalic acid using a re-anodizing technique, Appl. Surf. Sci. 236: 270–277. https://doi.org/10.1016/j.apsusc.2004.04.030.
19. **Aerts, T.; Jorcin, J.-B.; De Graeve, I.; Terryn, H.** 2010. Comparison between the influence of applied electrode and electrolyte temperatures on porous anodizing of aluminium, Electrochim. Acta 55: 3957–3965. https://doi.org/10.1016/j.electacta.2010.02.044.
20. **Bartolome, M.;. Lopez, V.; Escudero, E.; Caruana, G.; Gonzalez**, **J.** 2006. Changes in the specific surface area of porous aluminium oxide films during sealing, Surf. Coat. Technol. 200: 4530–4537. https://doi.org/10.1016/j.surfcoat.2005.03.019.
21. **Bartolome, M. J.; J. F. del Rio; Escudero, E.; S. Feliu, Jr.; Lopez, V.; Otero, E.; Gonzalez, J. A.** 2008. Behavior of different bare and anodised aluminium alloys in the atmosphere, Surf. Coat. Technol. 202: 2783–2793. https://doi.org/10.1016/j.surfcoat.2007.10.019.

22. **Moylan S. P. l.; Kompelle, S.; Chandrasekar, S.; Farris, T. N.** 2001. A Nano- Indentation Study of Mechanical Properties of Thin Surface Layers Affected by Manufacturing Processes, in: G. Dalmaz, A. A. Lubrecht, D. Dowson, M. Priest (Eds.), Tribology Research: From Model Experiment to Industrial Problem, A Century of Efforts in Mechanics, Materials Science and Physico-Chemistry, Elsevier Amsterdam, 895–903.
23. **Chicot, D.; Demarecaux, P.; Lesage, J.** 1996. Apparent interface toughness of substrate and coating couples from indentation tests, Thin Solid Films 283: 151–157. https://doi.org/10.1016/0040-6090(96)08763-9.
24. **Ko, S.; Lee, D.; Jee, S.; Park, H.; Lee, K.; Hwang, W.** 2004. Mechanical properties and residual stress measurements in anodic aluminium oxide structures using nanoindentation, Glass Phys. Chem. 31 (2005) 356–363, meeting of the European-Ceramic-Society, St Petersburg, RUSSIA, JUL 05-07. https://doi.org/10.1007/s10720-005-0069-x.
25. **Dalmas, D.; Benmedakhene, S.; Richard, C.; Laksimi, A.; Beranger, G.; Gregoire, T.** 2001. Characterization of adherence and cracking within coated materials by an acoustic emission method: application to a WC-Co coating on a steel substrate, Comptes Rendus Acad. Sci. Ser. II C 4: 345–350. https://doi.org/10.1016/S1387-1609(01)01240-3.
26. **Pelletier, H.; Krier, J.; Mille, P.** 2006, Characterization of mechanical properties of thin films using nanoindentation test, Mech. Mater. 38: 1182– 1198. https://doi.org/10.1016/j.mechmat.2006.02.011.
27. **Raid, A.; Boualem, N.; Fridrici, V.; Kapsa, Ph.** 2011. Wear fretting behavior of thick HA anodizing alumina layer, MECHANIKA. 17(4): 444-448. https://doi.org/10.5755/j01.mech.17.4.578.
28. **Ma, Y.; Zhou, X.; Thompson, G. E.; Curioni, M.; Zhong, X.; Koroleva, E.; Skeldon, P.; Thomson, P.; Fowles, M.** 2011. Discontinuities in the porous anodic film formed on AA2099-T8 aluminium alloy, Corrosion Sci. 53: 4141–4151. https://doi.org/10.1016/j.corsci.2011.08.023.
29. **Torkar, M.; Godec, M.; Lamut, M.** 2009. Origin of stains on anodized aluminium profile, Eng. Fail. Anal. 16: 909–913. https://doi.org/10.1016/j.engfailanal.2008.08.021.
30. **Fares, C.; Boukharouba, T.; Belouchrani, M.; Britah, A.; Abdelaziz, M. N.** 2009. Determination of the Hardness of the Oxide Layers of 2017a Alloys, in: T. Boukharouba, M. Elboujdaini, G. Pluvinage (Eds.), Damage and Fracture Mechanics, Springer Netherlands, 1–10.

A. Raid, S. Pavan, V. Fridrici, C. Poilâne, Ph. Kapsa

TEMPERATURE EFFECT ON THE KINETIC ALUMINA LAYER GROWTH ON 5086 ALUMINUM SUBSTRATE

S u m m a r y

To achieve desired porous structure for specific applications, the film growth kinetics and nanostructure can be largely controlled by well monitoring anodization parameters. The pores distribution and dimensions can be significantly affected by the electrolyte nature, the applied voltage and the anodization temperature which seem to be one of the major parameters. In the present work, all specimens anodized with the same starting courant density value of 1.4 A were analyzed. The effects of Low (LT) and room (RT) temperatures on hard anodizing layers were studied qualitatively and quantitatively. At room temperature, the total current is maintained at high levels due to large reduction current that slows the growth of the oxide layer. For low temperature, the current decreases more rapidly against anodizing time which leads to thick alumina layer with high mechanical properties. The best results of anodized layer hardness both, on the surface and at the profile section were observed at 120 min anodizing time; beyond this time, the thickness increases up to 140 μm for 5 h but with lower proprieties due to porosity.

Keywords: aluminium, anodization, temperature, pore, hardness.

Received September 29, 2017
Accepted December 07, 2017